Optimal Operation of Ethylene Polymerization Reactors for Tailored Molecular Weight Distribution

M. Asteasuain, A. Brandolin

Planta Piloto de Ingeniería Química (Universidad Nacional del Sur—CONICET), Camino La Carrindanga km 7, C.C. 717, 8000 Bahía Blanca, Argentina

Received 18 September 2006; accepted 9 February 2007
DOI 10.1002/app.26295
Published online 11 May 2007 in Wiley InterScience (www.interscience.wiley.com).

ABSTRACT: This work presents a comprehensive steady-state model of the high-pressure ethylene polymerization in a tubular reactor able to calculate the complete molecular weight distribution (MWD). For this purpose, the probability generating function technique is employed. The model is included in an optimization framework, which is used to determine optimal reactor designs and operating conditions for producing a polymer with tailored MWD. Two application examples are presented. The first one involves maximization of conversion to obtain a given MWD, typical of industrial operation. Excellent agreement between the resulting MWD and the target one is achieved with a conversion about 5% higher than the ones commonly reported for this type of reactor. The second example consists in finding the design and operating conditions necessary to produce a polymer with a bimodal MWD. The optimal design for this case involves a split of the initiator, monomer, and modifier feeds between the main stream and two lateral injections. To the best of our knowledge, this is the first work dealing with the optimization of this process in which a tailored shape for the MWD is included. © 2007 Wiley Periodicals, Inc. J Appl Polym Sci 105: 2621–2630, 2007

Key words: polyethylene (PE); radical polymerization; molecular weight distribution; modeling; optimization; tubular reactor

INTRODUCTION

Polyethylene is a commodity polymer with one of the most important markets among the commercial polymers, with a world annual production of about 35 million tons.[1] Low density polyethylene (LDPE), one of the members of the polyethylene family, is produced by high-pressure free-radical polymerization in tubular or autoclave reactors. This work focuses on the polymerization in tubular reactors to produce LDPE. This is a widely used industrial process, which is carried out under rigorous operating conditions. For instance, axial velocities are usually around 11 m/s, pressures range from 1800 to 2800 bar, and temperatures are between 50°C at the reactor entrance and 335°C at the peaks. A typical reactor has a main feed consisting of ethylene monomer, a mixture of modifiers, inert species, and oxygen initiator. In addition, there are lateral injections of peroxide initiator mixtures, which may be accompanied by monomer and/or modifiers. The reactor is divided in heating/cooling jacket zones to reach an appropriate reaction temperature or to control the exothermic reaction. Pressure pulsing of the reactor is sometimes applied to control polymer buildup at the reactor walls.

Driven by commercial reasons, several studies have been performed on the optimization of LDPE tubular reactors, most of which used simplified models. For instance, Mavridis and Kiparissides[2] presented an optimization strategy using a theoretical model to find the best values of the operative parameters, so as to obtain the maximum conversion for a polyethylene of a certain molecular weight. Yoon and Rhee[3] determined optimal temperature profiles that maximized conversion. They used a simplified model without including requirements on molecular properties. Kiparissides et al.[4] carried out an online optimization of a LDPE tubular reactor taking into account requirements on the polymer melt index and density. In a series of papers,[5,6] a rigorous model of the reactor was used to determine optimal operating policies and reactor design features for an industrial reactor, while keeping average molecular properties within desired values.

A very important molecular property to which less attention has been paid is the complete molecular weight distribution (MWD). Optimization of the reactor operation while tailoring the MWD is a very useful application of a mathematical model, because a number of processing and end-use properties of the polymer are strongly dependent on the breadth and shape of the MWD. For example, high molecular

Correspondence to: Adriana Brandolin (abrandolin@plapiqui.edu.ar).

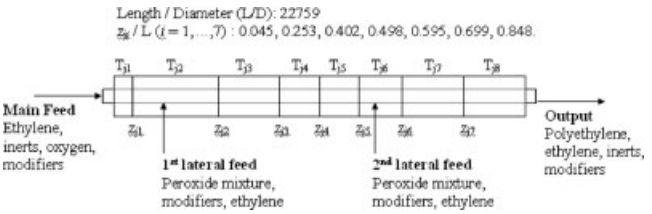

Figure 1 Tubular reactor for high-pressure ethylene polymerization.

weight tails and shoulders can increase the sensitivity of melt viscosity to shear rate.[7] Several methods have been proposed to predict the complete MWD in different systems. However, applications for tailoring the MWD are not frequent. In the case of the high-pressure ethylene polymerization in tubular reactors, there are some works dealing with the calculation of the complete MWD,[1,7–9] but few of them attempted to tailor this property in an optimization framework.[9]

This work presents a detailed description of a comprehensive steady-state model of the high-pressure ethylene polymerization in a tubular reactor that is able to calculate the complete MWD as function of the reactor axial distance. Furthermore, its application in optimizing the reactor operation while producing a polymer with tailored MWD is presented.

A previous model[10] is extended to calculate the complete MWD by means of the probability generating function (PGF) technique developed by the authors.[11–13] This technique allows modeling the MWD easily and efficiently, in spite of the complexity of the reactor model. Detailed modeling capabilities of the previous model are retained. The rigorous model of the polymerization reactor presented here is implemented in the gPROMS (Process Systems Enterprise, Ltd.) optimization environment. Optimizations to determine optimal operating conditions for producing a polymer with specific MWD were performed using this tool. To the best of our knowledge, this is the first work dealing with the optimization of this process in which a tailored shape for the MWD is included. Two application examples are presented. The first one involves maximization of conversion for a given MWD, and the second one consists in finding the operating conditions necessary to produce a polymer with a bimodal MWD.

MODEL DESCRIPTION

The reactor configuration is displayed in Figure 1. It corresponds to a typical industrial reactor, with eight jacket zones and two lateral feeds. Some of the design features, such as the length-to-diameter ratio or the relative lengths of each jacket zone, are also shown in Figure 1. The mathematical model of the polymerization reactor is based on a previous, comprehensive model developed by the authors,[10] which is extended in this work to calculate the complete MWD. It assumes plug flow and supercritical reaction mixture. Besides, it considers variation of physical and transport properties (i.e., axial velocity, heat capacity, thermal conductivity, viscosity, and density) along the axial distance, calculated with rigorous correlations. Detailed calculation of the heat-transfer coefficient along the axial distance is also included.[14]

Average molecular weights, MWD, and short and long chain branches are key molecular parameters in defining the properties of LDPE. In this work, focus is placed on the complete MWD and the average molecular weights. Therefore, only the reactions of the former kinetic mechanism[10] that are crucial for the prediction of the mentioned properties, as well as the conversion and temperature profiles, are retained. The kinetic mechanism is shown in Table I.

To avoid iterative calculations that increase the computational burden, the jacket temperature at each one of the eight reaction zones is assumed constant,

TABLE I
Kinetic Mechanism

Peroxide initiation

$$\mathrm{I}_k \xrightarrow{k_{ik}} 2\mathrm{R}(0)\ k = 1,2 \quad (1)$$

Oxygen initiation

$$\mathrm{O}_2 + \mathrm{M} \xrightarrow{k_0} 2\mathrm{R}(0) \quad (2)$$

Monomer thermal initiation

$$3\mathrm{M} \xrightarrow{k_{mi}} \mathrm{R}(1) + \mathrm{R}(2) \quad (3)$$

Generation of inert

$$\mathrm{O}_2 + \mathrm{R}(m) \xrightarrow{f_0 k_0} \mathrm{X} \quad (4)$$

Propagation

$$\mathrm{R}(m) + \mathrm{M} \xrightarrow{k_p} \mathrm{R}(m+1) \quad (5)$$

Termination by combination

$$\mathrm{R}(n) + \mathrm{R}(m) \xrightarrow{k_{tc}} \mathrm{P}(n+m) \quad (6)$$

Thermal degradation

$$\mathrm{R}(m) \xrightarrow{k_{tdt}} \mathrm{P}(m) + \mathrm{R}(0) \quad (7)$$

Chain transfer to monomer

$$\mathrm{R}(m) + \mathrm{M} \xrightarrow{k_{trm}} \mathrm{P}(m) + \mathrm{R}(1) \quad (8)$$

Chain transfer to polymer

$$\mathrm{R}(n) + \mathrm{P}(m) \xrightarrow{mk_{trp}} \mathrm{P}(n) + \mathrm{R}(m) \quad (9)$$

Chain transfer to modifier

$$\mathrm{R}(m) + \mathrm{S} \xrightarrow{k_{trs}} \mathrm{P}(m) + \mathrm{R}(0) \quad (10)$$

and the pressure pulse is neglected. The peroxide mixtures are treated as single fictitious species. The same is done for the modifier mixtures. These simplifications were validated in a previous work by the authors[15] against several data sets from an industrial tubular reactor. The same modifier mixture, and therefore the same single fictitious modifier, that is employed for the main reactor feed is considered for possible lateral feeds. However, peroxide mixtures for the first and second lateral feeds are different in composition,[15] and hence they are represented in this model by two different fictitious peroxides (I_1 for the first lateral feed and I_2 for the second one). The set of kinetic constants obtained in Asteasuain et al.[15] is used here. The main model equations are listed in the Appendix.

As mentioned earlier, the LDPE reactor model implementation and process optimization are carried out in gPROMS. To comply with software requirements for optimization activities, the lateral feeds to the reactor are included as part of the mass and energy balance equations of the reactor model (terms involving $\overline{F}_j$ in eqs. (A1), (A2), and (A7)). The instantaneous inlet of mass and energy represented by a lateral feed is modeled by means of a flow per unit length ($\overline{F}_j(z)$). This flow is nonzero only within a small Δz starting at the lateral inlet position ($z_{i\text{th lateral feed}}$). Values of $\overline{F}_j$ and Δz must verify

$$\int_{z_{i\text{th lateral feed}}}^{z_{i\text{th lateral feed}}+\Delta z} \overline{F}_j(z) M_{wj} dz = F_{j,i\text{th lateral feed}} \qquad (11)$$

where $F_{j,i\text{th lateral feed}}$ is the mass flow of component j at the ith lateral feed. A value of $\Delta z = 10^{-3}$ m was found to be appropriate so that model outputs with this approach coincide with simulation results of a FORTRAN version of the model in which instantaneous (regarding axial position) lateral feeds are considered.

The main contribution of the present model is the addition of the calculation of the complete MWD along the axial distance. The MWD is calculated, independently, in number, weight, and chromatographic fractions. The latter is a magnitude proportional to the mass times the molecular weight, and therefore is equivalent to the differential MWD as defined in the ASTM Standard D 3593-80 for size-exclusion chromatography representation of the MWD. The MWD prediction is performed by means of the PGF technique developed by the authors.[11–13] With this technique, first the mass balances of the generic macromolecular species ($R(m)$ and $P(m)$) are transformed into the PGF domain, obtaining the balance equations for the corresponding PGFs ($\phi_{a,l}$ and $\varphi_{a,l}$). The expressions corresponding to these equations are shown in the Appendix. Then, the complete MWDs are obtained by means of an appropriate numerical inversion of the PGFs. The inversion step is represented by the function $f(\varphi_{a,l}(z))$ in eqs. (A12)–(A14) in the Appendix. This function stands for a set of algebraic equations for calculating the MWD as a linear combination of the PGF at different values of the dummy variable l. The inversion procedure employed in this work is the Stehfest's algorithm.[12] The PGF technique allowed modeling the MWD easily and efficiently, in spite of the complexity of the reactor model. The resulting model also keeps the capabilities of the former model to calculate the following quantities along the axial distance: monomer conversion, reaction mixture temperature and pressure, mass fraction of oxygen, peroxides, monomer, radicals and polymer; average molecular weights; Peclet, Nusselt, Reynolds, and Prandtl numbers; global heat-transfer coefficient, velocity, viscosity, and specific heat.

OPTIMIZATION OF THE LDPE TUBULAR REACTOR

For comparison purposes, temperature profiles, MWD, and the average molecular weights of a typical industrial run are used. Operating and design conditions corresponding to this run are presented in Table II as the base case. Other design conditions are shown in Figure 1.

First case study

The first case study involves a maximization of conversion while achieving a prespecified MWD. This target MWD is selected to be same as the base case one. By these means useful comparisons can be performed between the obtained operating and design conditions and the typical industrial ones of the base case. A set of 19 optimization variables is considered, involving flow rates of different components in the main and lateral feeds, the inlet temperature and pressure, and location of the lateral feeds. Optimization variables are listed in Table II. All of these variables are ''time invariant'' from the point of view of the optimization problem, that is, they are constant with respect to the independent variable (reactor axial length) in the differential-algebraic equation system (DAE). Two optimization problems are solved: in the first one the lateral feeds are assumed to be at the same temperature of the main feed stream (*cold* lateral feeds); in the second, the temperature of the feeds is assumed to be equal to the reactor temperature at the injection point (*hot* lateral feeds). The maximum allowed deviation with respect to the original MWD is specified by adding the constraints shown in eqs. (12) and (13) to the optimization problem.

TABLE II
Optimal Operating Conditions: First Case Study

Variable	Base case	Optimal
Inlet temperature (°C)	77	72
Inlet pressure (bar)	2300	2800
Oxygen flow rate (kg/s)	6.9×10^{-5}	7.7×10^{-5}
Modifier flow rate (kg/s)	0.00762	0.2
Peroxide flow rate: 1st inj. (kg/s)	0.00102	6.1×10^{-4}
Peroxide flow rate: 2nd inj. (kg/s)	1.57×10^{-4}	8.3×10^{-5}
Monomer flow rate: Main feed (kg/s)	11	11
Monomer flow rate: 1st inj. (kg/s)	0	0
Monomer flow rate: 2nd inj. (kg/s)	0	0
Location of 1st injection (z/L)	0.121	0.037
Location of 2nd injection (z/L)	0.636	0.631
Jacket temperature: zones 1–8 (°C)	170–225–170–170–170–170–170–170	153–229–150–150–150–150–150–150
Conversion	25%	30%

$$\sum_i \left(\frac{w_{\text{new}}(m_i, z_{\max}) - w_{\text{base case}}(m_i)}{w_{\text{base case}}(m_i)} \right)^2 \leq 0.01 \qquad (12)$$

$$\sum_i \left(\frac{c_{\text{new}}(m_i, z_{\max}) - c_{\text{base case}}(m_i)}{c_{\text{base case}}(m_i)} \right)^2 \leq 0.01 \qquad (13)$$

Only 26 points of the MWD, covering a chain length range between 10 and 100,000, are considered in the summations of eqs. (12) and (13). These points are approximately equally spaced in a log scale basis. In this way, a good level of detail in the shape of the MWD is achieved while maintaining a reasonable size of the mathematical model.

An upper bound is imposed on the reaction mixture temperature along the axial distance to ensure safe operating conditions (thermal runaway occurs at 345°C):[4]

$$T(z) \leq 335°\text{C} \qquad (14)$$

Besides, an upper bound is also considered for the reactor temperature at the reactor exit, required for downstream process units:

$$T(z_{\max}) \leq 285°\text{C} \qquad (15)$$

A constraint in the total monomer fed to the reactor (main feed plus lateral feeds) is applied, so as to keep the same flow rate as in the base case:

$$A\left(F_{\text{M,main}} + \int_0^z \overline{F}_{\text{M}}(z) M_{w\text{M}} dz \right) = 11 \text{ kg/s} \qquad (16)$$

where A is the cross-sectional area of the reactor.

Lower and upper bounds for the optimization variables are selected according to the usual operating conditions of an industrial reactor. Finally, the optimization problem involves maximizing conversion at the reactor exit ($x(z_{\max})$) subject to the reactor model and the constraints shown in eqs. (12)–(16). The optimization, which only includes ''time''-invariant optimization variables, is solved using the commercial software gPROMS. The employed optimization solver integrates the DAE system at each iteration of the optimization algorithm. A DAE solver that is based on variable time step/variable order backward differentiation formulae (BDF) is used for the integration of the model equations and their sensitivity equations at all iterations. The optimization solver implements a single shooting algorithm, which means that a single integration of the dynamic model over the entire horizon is performed for each evaluation of the objective function. The nonlinear programming problem is solved by means of a sequential quadratic programming method.[16]

Second case study

The second case study aims at designing the process to tailor the MWD. A bimodal distribution is selected as the target distribution because it constitutes a challenge, since it is not obtained under usual operating conditions. For instance, in a set of 31 operating cases taken from an actual industrial reactor, only polyethylene with monomodal distribution is produced. To show the flexibility of this approach to determine the target MWD, only the existence of a local minimum, a necessary condition for a bimodal distribution, and its approximate location are specified. This is performed by including eqs. (17) and (18) in the optimization problem, which ensures that a minimum occurs within the interval $[m_1,m_3]$, with $m_1 < m_2 < m_3$. Chain length values m_1, m_2, and m_3 are selected so that the corresponding molecular weights (m_i $M_{w\text{M}}$) are, respectively, 44,380, 224,000, and 280,000 g/mol. The interval $[m_1,m_3]$ defined with these values corresponds to the region between the peak and the high molecular weight shoulder of

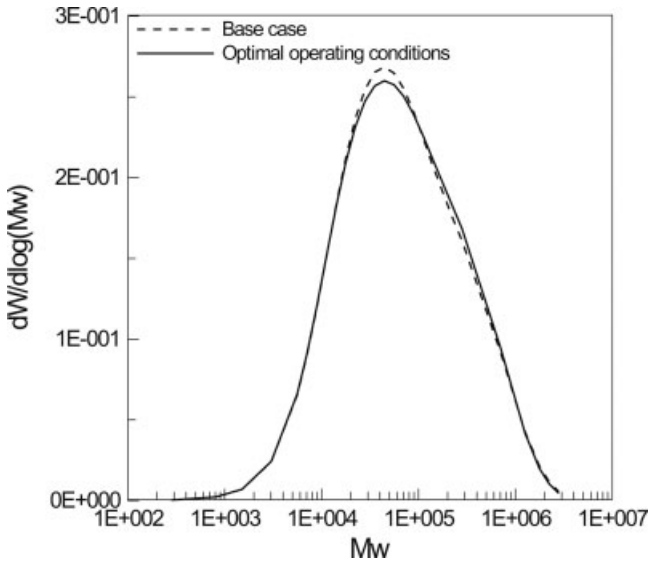

Figure 2 Comparison of the original and final MWD (first case study).

the base case distribution (see Fig. 2). Due to the presence of the shoulder, this region would be prone to show the peaks of a bimodal distribution. The value of m_2 is arbitrarily selected between m_1 and m_3. The aim of the optimization problem is to minimize the objective function shown in eq. (19), with the purpose of increasing the height of the shoulder of the distribution.

$$c(m_2, z_{\max}) - c(m_1, z_{\max}) \leq 0 \tag{17}$$

$$c(m_2, z_{\max}) - c(m_3, z_{\max}) \leq 0 \tag{18}$$

$$\mathrm{FO} = c(m_2, z_{\max}) - c(m_3, z_{\max}) \tag{19}$$

Equations (17) and (18) replace eqs. (12) and (13) in the optimization formulation of the first case study. Besides, a lower bound on the monomer conversion is added to avoid uneconomical operation:

$$x(z_{\max}) \geq 0.2 \tag{20}$$

The same set of optimization variables as in the previous case is used, plus the possibility of including modifier in the lateral injections.

RESULTS AND DISCUSSION

Optimization results for the first case study are shown in Table II. It may be seen that the monomer conversion is higher than in the base case. The success in obtaining the target MWD can be observed in Figure 2, which depicts the desired MWD (base case MWD) and the one obtained for the optimal design. MWD is plotted as the differential MWD (ASTM Standard D 3593-80 for size-exclusion chromatography), which may be more familiar to the general reader, but it should be kept in mind that it is equivalent to the chromatographic fraction ($c(m)$) employed in the model. An even closer match is obtained for the MWD expressed in weight fraction ($w(m)$).

Figure 3 shows the temperature profiles corresponding to the base case and to the optimal operating conditions. Notice that the path and end point constraints (with respect to the axial length) on the reactor temperature (eqs. (14) and (15)) are satisfied.

Optimization results are the same when using *cold* or *hot* lateral feeds. This is a reasonable result, because the optimal point involves lateral addition of initiator only. Since this addition involves a very small amount of mass, it does not contribute significantly to the reaction mixture enthalpy. Notice that all the monomer is fed in the main stream, and that the first injection point in now placed nearer the reactor entrance. These results are consistent with previous studies by the authors regarding a parametric analysis of the influence of different operating variables on this process.[6]

The optimal solution shows a high inlet pressure, which is one of the main factors in maximizing the conversion. For instance, if all operating variables are maintained at the optimal operating point, but the inlet pressure is kept at the base case value, the final conversion is 24% instead of 30%. The initiator flow rates are also critical to the conversion level, as

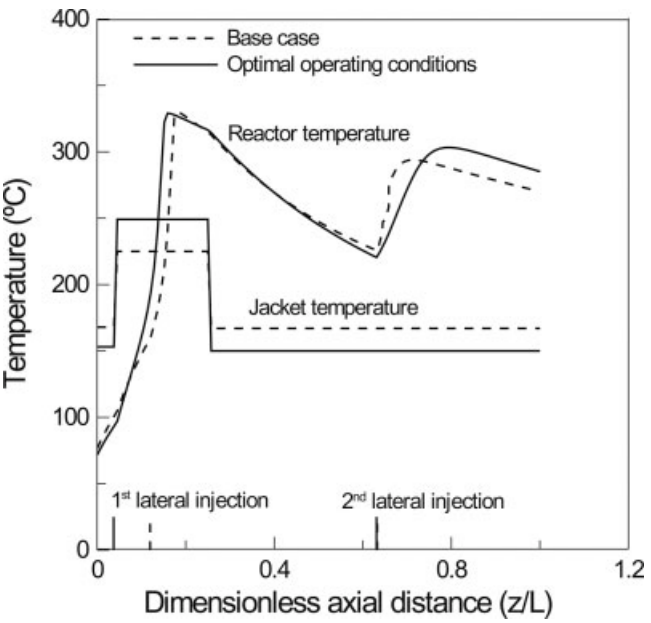

Figure 3 Temperature profiles corresponding to the base case and to the optimal operating conditions (first case study).

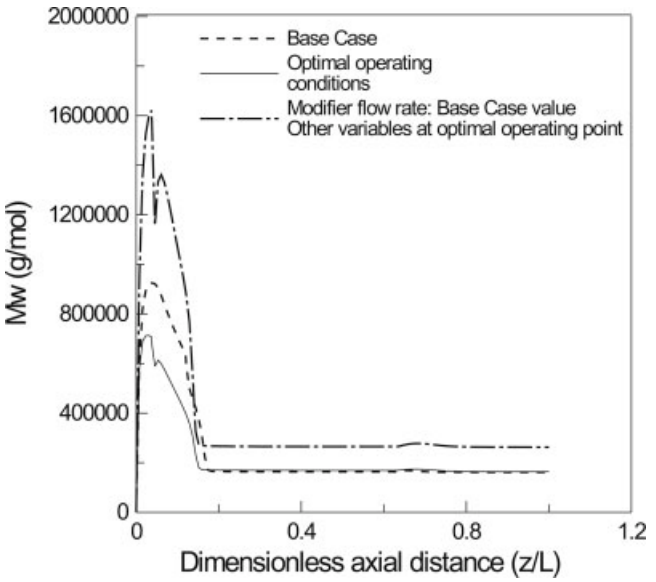

Figure 4 Influence of the modifier flow rate on Mw for the optimal operating point (first case study).

these species are the main source of radicals for the polymerization reaction. On the other hand, oxygen flow rate and inlet temperature do not produce significant effects, since conversion remains around 30% when these variables are left at their base case values.

The main effect of the increase in modifier flow rate is to compensate the rise in polymer molecular weight produced by the changes in the other operating conditions. This is exemplified in Figure 4. It depicts the M_w along the axial distance for three different operating conditions: those of the base case, those of the optimal operating point, and a case where the modifier flow rate is at the base case value while other operating variables remain at their optimal point values. It may be seen that, if the modifier flow rate is kept at its base case value, the polymer molecular weight is significantly higher, particularly in the first reaction zone (approximately up to $z/L = 0.3$). Then, with the optimal value of the modifier flow rate, the molecular weight is driven to the desired value of the base case polymer. As expected, these changes in the modifier flow rate have a negligible effect on monomer conversion.

Figure 5 shows the resulting MWD for the second case study. A comparison of the distributions after the first reaction zone and at the reactor exit is presented. A clear bimodality at the reactor exit can be observed, showing the success of the optimization procedure. The set of optimal operating conditions are shown in Table III. The operating scenario is very different from the base case and also from the optimal one obtained for the first case study. Notice that now the monomer feed is split between the main feed and two lateral injections. Side injections of modifiers are also used, with an important addition in the second injection. This radical change in the process conditions is not unexpected since a polymer with a very different MWD is seeked. Other authors[1] have also found that lateral additions of modifiers are necessary to obtain bimodal MWDs in tubular reactors.

As shown in Figure 5, the high molecular weight polymer formed after the first lateral injection contributes to the right peak of the distribution, while the lower molecular weight polymer produced after the second injection (which involves an important addition of modifier) is responsible for the left peak of the distribution. Figure 6 shows that a low reaction temperature predominates through a long first reaction zone, and a high temperature in the second reaction zone. This temperature profile is a key factor for producing the high molecular weight polymer in the first reaction zone, and the low molecular weight polymer in the second one. The jacket temperature is increased towards the end of the first reaction zone, to raise the reactor temperature to a level that will allow achieving a suitable conversion value. Similarly, an increase in the jacket temperature is observed towards the end of the second reaction zone, to avoid an excessive cooling of the reactor. The main effect of the split of the monomer feed is to aid in lowering the reactor temperature in the first reaction zone. Since this split reduces the monomer concentration in this zone, the reaction rate, and consequently the heat generation, is lowered.

The first lateral injection is at a similar position as the one obtained in the optimal point of the first case. However, the second one is moved towards the

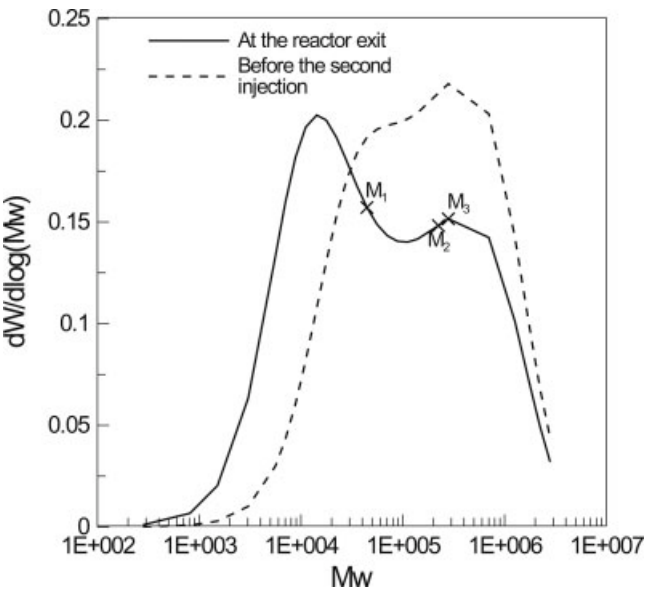

Figure 5 Bimodal MWD (second case study).

TABLE III
Optimal Operating Conditions: Second Case Study

Variable	Base case	Optimal
Inlet temperature (°C)	77	70
Inlet pressure (bar)	2300	2800
Oxygen flow rate (kg/s)	6.9×10^{-5}	5.9×10^{-5}
Modifier flow rate: main feed (kg/s)	0.00762	0.12
Modifier flow rate: 1st inj. (kg/s)	0	3.5×10^{-3}
Modifier flow rate: 2nd inj. (kg/s)	0	0.9
Peroxide flow rate: 1st inj. (kg/s)	0.00102	2.4×10^{-4}
Peroxide flow rate: 2nd inj. (kg/s)	1.57×10^{-4}	8.6×10^{-5}
Monomer flow rate: main feed (kg/s)	11	9.4
Monomer flow rate: 1st inj. (kg/s)	0	0.6
Monomer flow rate: 2nd inj. (kg/s)	0	1
Location of 1st injection (z/L)	0.121	0.031
Location of 2nd injection (z/L)	0.636	0.377
Jacket temperature: zones 1–8 (°C)	170–225–170–170–170–170–170–170	154–150–270–226–176–170–270–270
Conversion	25%	25%

high temperature zone of the reactor. This evidently contributes to the formation of the low molecular weight polymer. Besides, the high modifier flow rate of this feed also aids in obtaining the low molecular weight material.

CONCLUSIONS

In this work a detailed mathematical model of the high-pressure ethylene polymerization in a tubular reactor is presented. The model is able to calculate conversion and temperature profiles as well as the concentration of the reactive species. Application of the PGF technique to the mass balances makes it possible to calculate the complete MWD with no previous assumption on the distribution shape. This model is successfully included in an optimization framework that allows the determination of the reactor operating and design conditions for the production of polymers with tailored MWD.

The optimization approach presented in this paper allows great flexibility for specifying the target MWD and other process constraints. Two case studies are presented. The first one involves maximization of conversion for a given MWD. The optimization procedure is able to find a combination of operating and design conditions appropriate to obtain a conversion higher than the ones reported for typical industrial operations, while keeping the variables within safe operating ranges. Inlet pressure as well as initiator flow rates and lateral injection locations are the key variables in maximizing conversion. Furthermore, the modifier flow rate in the main stream is crucial for achieving the desired MWD.

In the second case the optimization succeeds in tailoring a complex MWD shape. Bimodality is obtained by means of an appropriate temperature profile together with the splitting of the monomer and modifier feeds between the main stream and two lateral injections. The appropriate combination of these factors produces fractions of high and low molecular weight polymer in the first and second reaction zones, respectively.

In brief, the combination of the mathematical model with the optimization approach presented in this work constitutes a tool of academic and technological interest. The results presented show that it is possible to gain insight on the complex relationships between process variables and product quality.

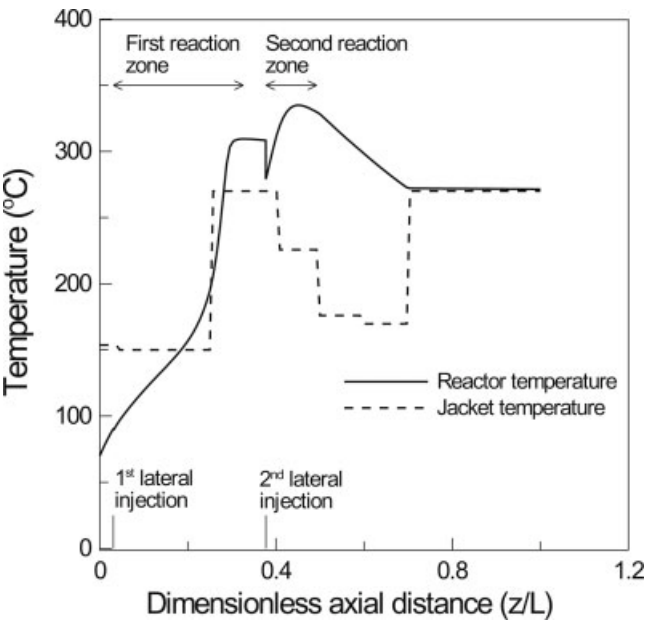

Figure 6 Temperature profiles corresponding to the optimal operating conditions of the second case study.

NOMENCLATURE

A	cross-sectional area of the reactor
$c(m)$	chromatographic fraction of the macromolecule of chain length m
$c_{\text{base case}}(m_i)$	chromatographic fraction of the macromolecule of chain length m_i for the base case operating conditions and reactor design
$c_{\text{new}}(m_i,z)$	chromatographic fraction of the macromolecule of chain length m_i, at the axial position z, for the new operating conditions and reactor design
C_j	molar concentration of component j
C_p	heat-capacity of the reaction mixture
$\hat{C}_p$	monomer heat-capacity at the average temperature between the lateral feed temperature and the reactor temperature
D	reactor internal diameter
f_f	friction factor
$F_{j,i\text{th lateral feed}}$	mass flow of component j at the ith lateral feed
$\overline{F}_j$	molar flow per unit length of component j
F_{main}	global mass flow at the reactor entrance
$F_{\text{M,main}}$	monomer mass flow at the reactor entrance
I	peroxide initiator
L	reactor length
M	ethylene monomer
Mw	polymer weight average molecular weight
Mw_j	molecular weight of the j component
$n(m)$	number fraction of the macromolecule of chain length m
O_2	oxygen
P	reactor pressure
P(m)	polymer molecule of chain length m
R(m)	living radical of chain length m
r_j	generation rate of the j component
r_{pm}	reaction rate of the propagation reaction
S	modifier
T	reactor temperature
T_j	jacket temperature
T_{inlet}	reactor inlet temperature
U	global heat-transfer coefficient
v	axial velocity
$w(m)$	weight fraction of the macromolecule of chain length m
$w_{\text{base case}}(m_i)$	weight fraction of the macromolecule of chain length m_i for the base case operating conditions and reactor design
$w_{\text{new}}(m_i,z)$	weight fraction of the macromolecule of chain length m_i, at the axial position z, for the new operating conditions and reactor design
X	inert molecule
$z_{i\text{th lateral feed}}$	axial position of the ith lateral feed
z_{max}	axial position of the reactor exit

Greek letters

ΔH	enthalpy of the propagation reaction
$\phi_{a,l}$	probability generating function (PGF) of the radical chain length distribution. Subscript $a = 0, 1, 2$ stands for the MWD expressed in number, weight and chromatographic (mass times the molecular weight) fraction, respectively; subscript l is the dummy variable of the PGF
$\varphi_{a,l}$	PGF of the polymer chain length distribution. Subscripts a and l have the same meaning as for $\phi_{a,l}$
λ_a	ath order moment of the radical chain length distribution
μ_a	ath order moment of the polymer chain length distribution
ρ	density of the reaction mixture

APPENDIX: MAIN MODEL EQUATIONS

Global mass balance:

$$\rho(z)v(z) = F_{\text{main}} + \int_0^z \left(\sum_j \overline{F}_j(z) M_{w,j} \right) dz \qquad \text{(A.1)}$$

The global mass balance is formulated as an algebraic equation instead of a differential equation, because this resulted in better numerical behavior at the lateral injection points. The first right hand side term (F_{main}) is the contribution of the main reactor inlet to the total mass flow. The second term is the contribution of the lateral feeds encountered up to the axial distance z. This is straightforward from the explanation of the modeling of the lateral feeds given in the MODEL DESCRIPTION section.

Mass balances of components:

$$\frac{d(C_j(z)v(z))}{dz} = r_j(z) + \overline{F}_j(z) \qquad j = O_2, M, I_k(k = 1, 2), S \qquad \text{(A.2)}$$

where $\overline{F}_j(z)$ is the contribution of the lateral feeds. Expressions corresponding to the generation rates of the different components (r_j) can be found elsewhere.[10]

Balance equation for the ath order moment of the polymer MWD ($a = 0, 1, 2$):

$$\frac{d(\mu_a(z)v(z))}{dz} = \frac{1}{2}k_{tc}(z)\sum_{j=0}^{a}\binom{a}{j}\lambda_j(z)\lambda_{a-j}(z) + k_{tdt}(z)\lambda_a(z) + k_{trs}(z)S(z)\lambda_a(z) + k_{trp}(z)\mu_1(z)\lambda_a(z) - k_{trp}(z)\lambda_0(z)\mu_{a+1}(z) + k_{trm}(z)M(z)\lambda_a(z) \quad (A.3)$$

The right hand side of eq. (A.3) (as well as of eqs. (A.4)–(A.6)) corresponds only to the generation rate of the involved variable. There is no contribution of the lateral feeds since no polymeric species enter the reactor through these points.

Balance equation for the ath order moment of the radical MWD ($a = 0, 1, 2$):

$$\begin{aligned}\frac{d(\lambda_a(z)v(z))}{dz} &= k_0(z)\mathrm{O}_2(z)^{1.1}\mathrm{M}(z) + 2f_{I_1}k_{I_1}(z)I_1(z) \\ &+ 2f_{I_2}k_{I_2}(z)I_2(z) + k_p(z)\mathrm{M}(z)\sum_{j=0}^{a}\binom{a}{j}\lambda_j(z) \\ &- k_p(z)\mathrm{M}(z)\lambda_a(z) + k_{tdt}(z)\lambda_0(z) + k_{trs}(z)S(z)\lambda_0(z) \\ &+ k_{trm}(z)\mathrm{M}(z)\lambda_0(z) - k_{tc}(z)\lambda_0(z) - k_{tdt}(z)\lambda_a(z) \\ &- k_{trs}(z)S(z)\lambda_a(z) - k_{trm}(z)\mathrm{M}(z)\lambda_a(z) \\ &+ k_{mi}(z)\mathrm{M}(z)^3(1+2^a) - f_0k_0(z)\mathrm{O}_2(z)^{1.1}\lambda_a(z) \\ &- k_{trp}(z)\mu_1(z)\lambda_a(z) + k_{trp}(z)\lambda_0(z)\mu_{a+1}(z) \quad (A.4)\end{aligned}$$

In eqs. (A.3) and (A.4), $\mu_3 = (\mu_2/\mu_1)^3\mu_0$, as described in Brandolin et al.[10]

Balance equation for the PGF of the polymer MWD ($a = 0, 1, 2$):

$$\begin{aligned}\frac{d(\hat{\varphi}_{a,l}(z)v(z))}{dz} &= \frac{1}{2}k_{tc}(z)\sum_{j=0}^{a}\binom{a}{j}\hat{\phi}_{j,l}(z)\hat{\phi}_{a-j,l}(z) \\ &+ k_{tdt}(z)\hat{\phi}_{a,l}(z) + k_{trs}(z)S(z)\hat{\phi}_{a,l}(z) + k_{trp}(z)\mu_1(z)\hat{\phi}_{a,l}(z) \\ &- k_{trp}(z)\lambda_0(z)\hat{\varphi}_{a+1,l}(z) + k_{trm}(z)M(z)\hat{\phi}_{a,l}(z) \quad (A.5)\end{aligned}$$

Balance equation for the PGF of the radical MWD ($a = 0, 1, 2$):

$$\begin{aligned}\frac{d(\hat{\phi}_{a,l}(z)v(z))}{dz} &= k_0(z)\mathrm{O}_2(z)^{1.1}\mathrm{M}(z) + 2f_{I_1}k_{I_1}(z)I_1(z) \\ &+ 2f_{I_2}k_{I_2}(z)I_2(z) + k_p(z)\mathrm{M}(z)l\sum_{j=0}^{a}\binom{a}{j}\hat{\phi}_{j,l}(z) \\ &- k_p(z)M(z)\hat{\phi}_{a,l}(z) + k_{tdt}(z)\lambda_0(z) + k_{trs}(z)\mathrm{S}(z)\lambda_0(z) \\ &+ k_{trm}(z)\mathrm{M}(z)\lambda_0(z)l - k_{tc}(z)\lambda_0(z)\hat{\phi}_{a,l}(z) - k_{tdt}(z)\hat{\phi}_{a,l}(z) \\ &- k_{trs}(z)\mathrm{S}(z)\hat{\phi}_{a,l}(z) - k_{trm}(z)\mathrm{M}(z)\hat{\phi}_{a,l}(z) \\ &+ k_{mi}(z)\mathrm{M}(z)^3(1+2^al^2) - f_0k_0(z)\mathrm{O}_2(z)^{1.1}\hat{\phi}_{a,l}(z) \\ &- k_{trp}(z)\mu_1(z)\hat{\phi}_{a,l}(z) + k_{trp}(z)\hat{\varphi}_{a+1,l}(z) \quad (A.6)\end{aligned}$$

In eqs. (A.5) and (A.6), $\hat{\phi}_{a,l}(z) = \phi_{a,l}(z)\lambda_a(z)$, $\hat{\varphi}_{a,l}(z) = \varphi_{a,l}(z)\mu_a(z)$, and $\hat{\varphi}_{3,l}(z) = \frac{\hat{\varphi}_{2,l}(z)^2}{\hat{\varphi}_{1,l}(z)} + \hat{\varphi}_{2,l}(z) - \hat{\varphi}_{1,l}(z)$, as described by Asteasuain.[13]

Energy balance:

$$\rho(z)v(z)C_p(z)\frac{dT(z)}{dz} = -\frac{4U(z)(T(z)-T_j)}{D} + r_{pm}(z)(-\Delta H) + \hat{C}_p(T_{\text{inlet}} - T(z))\sum_j \overline{F}_j M w_j \quad (A.7)$$

where the last term of the right hand side of this equation represents the contribution of the lateral feeds.

Pressure drop:

$$\frac{dP(z)}{dz} = -\rho(z)\left(v(z)\frac{dv(z)}{dz} + \frac{2f_f v(z)^2}{D}\right) \quad (A.8)$$

Number average molecular weight:

$$Mn(z) = Mw_M\frac{\lambda_1(z)+\mu_1(z)}{\lambda_0(z)+\mu_0(z)} \quad (A.9)$$

Weight average molecular weight:

$$Mw(z) = Mw_M\frac{\lambda_2(z)+\mu_2(z)}{\lambda_1(z)+\mu_1(z)} \quad (A.10)$$

Monomer conversion:

$$x(z) = 1 - \frac{v(z)\mathrm{M}(z)}{F_{\mathrm{M},main} + \int_0^z \overline{F}_{\mathrm{M}}(z)\mathrm{M}w_M dz} \quad (A.11)$$

The integral in the denominator of this equation represents the monomer inlet through the lateral feeds encountered up to the axial position z.

Polymer MWDs:

$$n(m,z) = f(\varphi_{0,l}(z)) \quad (A.12)$$

$$w(m,z) = f(\varphi_{1,l}(z)) \quad (A.13)$$

$$c(m,z) = f(\varphi_{2,l}(z)) \quad (A.14)$$

where function $f(\varphi_{a,l}(z))$, $a = 0, 1, 2$, represents Stehfests inversion algorithm.

References

1. Kim, D.; Iedema, P. D. Chem Eng Sci 2004, 59, 2039.
2. Mavridis, H.; Kiparissides, C. Polym Proc Eng 1985, 3, 263.
3. Yoon, B. J.; Rhee, H. K. Chem Eng Commun 1985, 34, 253.
4. Kiparissides, C.; Verros, G.; Pertsinidis, A. Chem Eng Sci 1994, 49, 5011.
5. Brandolin, A.; Valles, E. M.; Farber, J. N. Polym Eng Sci 1991, 31, 381.
6. Asteasuain, M.; Ugrin, P. E.; Lacunza, M. H.; Brandolin, A. Polym React Eng 2001, 9, 163.

7. Wells, G. J.; Ray, W. H. Macromol Mater Eng 2005, 290, 319.
8. Schmidt, C.; Busch, M.; Lilge, D.; Wulkow, M. Macromol Mater Eng 2005, 290, 404.
9. Asteasuain, M.; Brandolin, A. International Symposium on Advanced Control of Chem Processes (ADCHEM 2006), Gramado, Brazil, 2006, pp. 235.
10. Brandolin, A.; Lacunza, M. H.; Ugrin, P. E.; Capiati, N. J. Polym React Eng 1996, 4, 193.
11. Asteasuain, M.; Sarmoria, C.; Brandolin, A. Polymer 2002, 43, 2513.
12. Asteasuain, M.; Brandolin, A.; Sarmoria, C. Polymer 2002, 43, 2529.
13. Asteasuain, M. Doctoral Thesis, Universidad Nacional del Sur, Bahía Blanca, Argentina 2003.
14. Lacunza, M. H.; Ugrin, P. E.; Brandolin, A.; Capiati, N. J. Polym Eng Sci 1998, 38, 992.
15. Asteasuain, M.; Pereda, S.; Lacunza, M. H.; Ugrin, P. E.; Brandolin, A. Polym Eng Sci 2001, 41, 711.
16. Process Systems Enterprise, Ltd, gPROMS v2.3.1 Introductory User Guide 2005.